2007-10

A Pseudospectral Observer for Nonlinear Systems

Ross, I. Michael; Gong, Qi; Kang, Wei

DISCRETE AND CONTINUOUS DYNAMICAL SYSTEMSSERIES B Volume 8, Number 3 (October 2007), p. 589-611
https://hdl.handle.net/10945/48635

DISCRETE AND CONTINUOUS
DYNAMICAL SYSTEMS–SERIES B
Volume **8**, Number **3**, October **2007**

Website: http://AIMsciences.org

pp. **589–611**

A PSEUDOSPECTRAL OBSERVER FOR NONLINEAR SYSTEMS

Qi Gong

Department of Electrical & Computer Engineering
University of Texas at San Antonio, San Antonio, TX 78249

I. Michael Ross

Department of Mechanical and Astronautical Engineering
Naval Postgraduate School, Monterey, CA, 93943

Wei Kang

Department of Applied Mathematics
Naval Postgraduate School, Monterey, CA, 93943

Abstract. In this paper, we present an observer design method for nonlinear systems based on pseudospectral discretizations and a moving horizon strategy. The observer has a low computational burden, a fast convergence rate and the ability to handle measurement noise. In addition to ordinary differential equations, our observer is applicable to nonlinear systems governed by deferential-algebraic equations (DAE), which are considered very difficult to deal with by other designs such as Kalman filters. The performance of the proposed observer is demonstrated by several numerical experiments on a time-varying chaotic nonlinear system with unknown parameters and a nonlinear circuit with a singularity-induced bifurcation.

1. **Introduction and problem formulation.** Observer design for nonlinear systems is one of the most important and difficult problems in control theory and its applications. Many results have been reported in the literature. Among them, observers based on a moving horizon have gained considerable attention [15, 10, 16, 18]. These observers are based on an online optimization algorithm that minimizes some selected measures of the estimation error. In contrast, other design methods are based on an off-line design of observer gains. Examples of such observers are high gain observers [4], backstepping observers [13], normal form observers [12, 14] and Extended-Kalman filters. Relative to the observer gain based approach, a main advantage of moving horizon observers using on-line optimization is that it is applicable to a wider variety of nonlinear systems. Furthermore, the manpower burden required to design and implement an on-line optimization-based observer is significantly reduced when compared to the gain-based methods because much of the tedious algebra derivations (such as changes of coordinates) required for by the gain-based observers is circumvented. This advantage is more pronounced for complex and nonlinear systems. Thus, the off-line design costs are significantly reduced

2000 *Mathematics Subject Classification.* Primary: 93E10, 93C10; Secondary: 93E11.

Key words and phrases. numerical observer, optimization, pseudospectral, nonlinear estimation.

The research was supported in part by NPS, the Secretary of the Air Force, and AFOSR under grant number, F1ATA0-60-6-2G002.

and the recurring costs are reduced even more substantially as the same observer algorithm is applicable, without much change, to different types of nonlinear systems. On the other hand, one of the main limitations of the on-line optimization-based methods is its requirement of real-time solutions to optimal control problems. Given that solving optimal control problems even in non-real-time is widely considered to be difficult, on-line optimization-based methods are not altogether popular. In recent years, however, pseudospectral (PS) methods [2, 21, 20, 22] have demonstrated that real-time solutions to optimal control problems are quite possible [20, 22]. This enabling new technology and the consistently rapid advance in the affordable high speed computation equipment facilitate a promising new observer using PS methods. In this paper, we prove some important results for the PS observer on its feasibility and convergence; we also demonstrate that the PS observer achieves a good balance between the computational load and the computational speed.

As a prelude for the problem formulation, consider the following nonlinear system with sampled output

$$\dot{x} = f(x,t) \tag{1}$$
$$y_i = h(x(t_i)) \tag{2}$$

where the state is $x \in \mathbb{R}^{N_x}$ and the output is $y \in \mathbb{R}^{N_y}$. It is assumed that $f : \mathbb{R}^{N_x} \times \mathbb{R} \to \mathbb{R}^{N_x}$ and $h : \mathbb{R}^{N_x} \to \mathbb{R}^{N_y}$ are continuously differentiable with respect to their arguments. Let $\{t_i\}_{i=0}^{\infty}$ be the sequence of sampling time satisfying $\lim_{i\to\infty} t_i = \infty$. Correspondingly, y_i is the measurement of the output $y(t)$ at the sampled points t_i. The observer problem is to estimate the state $x(t)$ at the current sampling time t_p based on the measurement $\{y_i\}_{i=0}^{p}$ and the system model. The state trajectory $x(t)$ is assumed to be bounded for all t. Note that (1) does not include a control input $u(t)$. However, the same method can be easily applied to controlled systems because $u(t)$ is a known function in the estimation process and thus the controlled system can be casted into the time-varying form (1).

Although the state $x(t)$ is not measured directly, in many applications we may have some information about it in addition to $y(t)$. For instance, $x(t)$ may only lie in a certain known region. Apparently, utilizing this information should help the design of the observer. For this reason we introduce the constraint

$$r(x(t)) \leq 0 \tag{3}$$

where $r : \mathbb{R}^{N_x} \to \mathbb{R}^{N_r}$ is continuously differentiable with respect to x. One essential purpose of the constraint set, $\{x \mid r(x) \leq 0\}$, is to capture any *a priori* known information. An important consequence of the constraint set is that we can include nonlinear systems governed by differential-algebraic equations (DAE). Observer design for DEAs is a challenging problem that cannot be dealt with by most of the existing results especially gain-based design. However, for the online optimization based methods, the appearance of the algebraic equations can simply be treated as constraint sets.

Another advantage of introducing this set is that a system may not be observable in the whole space, $\mathbb{R}^{N_x}$, but may be observable over some subset of $\mathbb{R}^{N_x}$. For

example, consider the system

$$\begin{aligned} \dot{x}_1 &= x_3 x_2 \\ \dot{x}_2 &= -x_3 x_1 \\ \dot{x}_3 &= 0 \\ y &= x_1 \end{aligned} \tag{4}$$

with given measurement $y(t) = \sin(t)$. Obviously, (x_2, x_3) can be either $(\cos(t), 1)$ or $(-\cos(t), -1)$. Therefore, (x_2, x_3) can not be determined based on measurement $y(t)$ alone. However, if we know that $x_3(t) > 0$, then the system is observable under the constraint.

The idea of constraint sets is also a key to handle the noise. It can be used to model the bounded disturbance/noise and utilize the stochastic information in the observer. In the later part of this paper we propose an algorithm to reduce the measurement noise based on the constraint set.

Throughout the paper the following observability condition is assumed.

Assumption 1. There is a constant $\delta > 0$ such that for any $T \in [\delta, \infty]$ and any two trajectories $x^1(t)$, $x^2(t)$ of (1) satisfying constraint (3),

$$\int_{T-\delta}^{T} \|h(x^1(t)) - h(x^2(t))\|^2 dt = 0$$

implies $x^1(t) = x^2(t)$, for all $t \in [T - \delta, T]$.

Remark 1. For a linear time-varying system $\dot{x} = A(t)x$, $y = C(t)x$, Assumption 1 always holds if the system is uniformly observable. In the nonlinear cases, if the system is uniformly observable in the sense of [4], Assumption 1 is automatically satisfied. This assumption also covers systems which are not uniformly observable such as (4) and the Duffing system discussed later in the paper.

Let $T = t_p$ be the current sampling time. Consider the following optimization problem:

Problem 1: Determine the function $z(t)$ that minimizes the cost function

$$J[z(\cdot)] = \int_{T-\delta}^{T} \|h(z(t)) - y(t)\|^2 dt \tag{5}$$

subject to the state equation

$$\dot{z}(t) = f(z(t), t) \tag{6}$$

and the constraint

$$r(z(t)) \leq 0 \tag{7}$$

Based on Assumption 1, Problem 1 has a *unique* optimal solution $z^*(t) = x(t)$. Therefore, the current state $x(T)$ can be obtained by evaluating the solution of Problem 1 at the current sampling time T, i.e., $x(T) = z^*(T)$. Based on this fact, a moving horizon type of observer can be constructed [15, 16, 10]. That is, at every sampling point, Problem 1 is solved online; then moving the time window $[T-\delta, T]$ to the next sampling point and the problem is solved again. The design philosophy is quite simple; however, a successful implementation of this concept depends on a key assumption: Problem 1 can be solved online.

To reduce the computational burden posed by moving horizon observers, a common method is to solve the online optimization problem recursively. This spreads the computational burden over time so that each iteration can be completed in real time. For example, in [15] an observer is constructed by searching a feasible solution making the cost function strictly decreasing. At every instance, no optimization needs to be done. Instead, the optimal solution is obtained as time advances to infinity. However, in [15] no discussion is given on how to find a feasible solution satisfying the requirement. Moreover, the continuous measurement is still required in contrast to our problem setting where only sampled measurements are utilized. In [16], a Newton's method is applied to a moving horizon observer, and the estimated states are given by a solution to a sequence of nonlinear algebraic equations. The observer may fail in the presence of noise since the nonlinear equations may fail to have a solution. Furthermore, as pointed out in [10], since an optimization algorithm could magnify an integration error, the requirement of accurate integration in [16] may worsen the situation. Thus, Kang [10] proposes to constructively combine numerical integration with optimization to design an observer based on a moving horizon strategy. The stability of such an observer can be proved under certain conditions identified in [10].

While the aforementioned methods can be applied to solve Problem 1, it is far more attractive to solve the problem directly, because if it can be solved, a finite-time nonlinear observer follows. The focus of this paper is to show that Problem 1 can be efficiently solved by Pseudospectral computational methods and the resulting PS numerical observer demonstrates some nice properties including: 1) The algorithm can be easily applied to a wide variety of nonlinear systems including systems governed by deferential-algebraic equations. It does not require specific system structure. 2) The performance of the observer is guaranteed. Indeed, the estimation error converges at a very fast rate (normally within several sampling periods). 3) It can be directly applied to continuous nonlinear systems with measurement noise and sampled output data. 4) The tuning of the observer is relatively simple.

The rest of the paper is organized as follows: in Section 2 we briefly present a PS discretization method and some fundamental results regarding the convergence of the PS methods. The proposed observer algorithm and its properties are discussed in Section 3 under several subsections. Numerical examples, including a family of chaotic Duffing systems and a nonlinear circuit governed by DAE, are also provided in this section. Finally, some concluding remarks are given in Section 4.

2. **Discretization and convergence.**

In this section, we prove some results on PS methods of solving optimal control problems that are relevant to the design of an observer. Additional details can be found in [5, 22, 2, 20]. We introduce the following assumption:

Assumption 2. Assume that the state $x(t)$ belongs to Sobolev space $W^{m,\infty}$ with $m \geq 2$. More specifically, for any $T \in [\delta, \infty)$, there is a constant $C > 0$ and an integer $m \geq 2$ such that

$$\sum_{i=0}^{m} \left|\left| \frac{d^{(i)}x(t)}{dt} \right|\right|_{L^\infty(T-\delta,T)} \leq C \tag{8}$$

where $d^{(i)}/dt$ denotes the i-th order distribution derivative. (A function $v'(t)$ is called the distributional derivative [1] of a L^1 function $v(t)$ if

$$\int_{T-\delta}^{T} v(t)\frac{d\phi(t)}{dt}dt = -\int_{T-\delta}^{T} v'(t)\phi(t)dt$$

for all smooth functions $\phi(t)$ with compact support in $[T-\delta, T]$.)

Remark 2. Note that, if $x(t)$ is C^1 and $\dot{x}(t)$ has bounded derivative everywhere except for a finite many points on the closed interval $t \in [T-\delta, T]$, then condition (8) is automatically satisfied. On the other hand, by Sobolev's Imbedding Theorems [1], any function $x(t)$ satisfying the aforementioned condition must have continuous $(m-1)$-th order classical derivatives on $[T-\delta, T]$. Therefore, this condition requires the optimal state $x(t)$ to be at least continuously differentiable. The condition can be further relaxed to cover the situation where $x(t)$ is only continuous but piecewise C^1; see [11] for details.

2.1. **Pseudospectral discretization.** We illustrate the ideas for a Legendre pseudospectral method while noting that much of the results apply to other PS methods as well. Since the Legendre PS method works on the interval $[-1, 1]$, we need to project the physical time domain $[T-\delta, T]$ in Problem 1 to the computational domain $[-1, 1]$. To this end, the following transformation is introduced

$$\tau = \frac{2t - 2T + \delta}{\delta} \tag{9}$$

Under (9), (6)-(7) are changed to

$$\frac{d\hat{z}(\tau)}{d\tau} = \frac{\delta}{2} f(\hat{z}(\tau), \frac{\tau\delta - \delta + 2T}{2}) \tag{10}$$

$$r(\hat{z}(\tau)) \leq 0 \tag{11}$$

where $\hat{z}(\tau) = z(\frac{\tau\delta-\delta+2T}{2})$. The cost function (5) is changed to

$$J[\hat{z}(\cdot)] = \frac{\delta}{2}\int_{-1}^{1} \|h(\hat{z}(\tau)) - \hat{y}(\tau)\|^2 d\tau$$

where $\hat{y}(\tau) = y(\frac{\tau\delta-\delta+2T}{2})$.

The basic idea of the Legendre PS method is to approximate $\hat{z}(\tau)$ by N-th order polynomials $z^N(\tau)$ based on Lagrange interpolation at the Legendre-Gauss-Lobatto (LGL) quadrature nodes, i.e.

$$\hat{z}(\tau) \approx z^N(\tau) = \sum_{k=0}^{N} z^N(\tau_k)\phi_k(\tau), \tag{12}$$

where τ_k are LGL nodes defined at follows.

$$\begin{array}{l} \tau_0 = -1, \ \ \tau_N = 1 \\ \tau_k, \text{ for } k = 1, 2, \ldots, N-1, \text{ are the roots of } \dot{L}_N(\tau) \end{array}$$

where $\dot{L}_N(\tau)$ is the derivative of the N-th order Legendre polynomial $L_N(\tau)$. The Lagrange interpolating polynomial $\phi_k(\tau)$ is defined by

$$\phi_k(\tau) = \frac{1}{N(N+1)L_N(\tau_k)}\frac{(\tau^2-1)\dot{L}_N(\tau)}{\tau - \tau_k}. \tag{13}$$

It is known that $\phi_k(\tau_j) = 1$, if $k = j$ and $\phi_k(\tau_j) = 0$, if $k \neq j$. The derivative of the i-th state $\hat{z}_i(\tau)$ at the LGL node τ_k can be approximated by

$$\dot{\hat{z}}_i(\tau_k) \approx \dot{z}_i^N(\tau_k) = \sum_{j=0}^{N} D_{kj} z_i^N(\tau_j),\ i = 1, 2, \ldots, N_x \tag{14}$$

where the $(N+1) \times (N+1)$ differentiation matrix D is defined by

$$D_{ik} \quad = \quad \begin{cases} \frac{L_N(\tau_i)}{L_N(\tau_k)} \frac{1}{\tau_i - \tau_k}, & \text{if } \ i \neq k; \\ -\frac{N(N+1)}{4}, & \text{if } \ i = k = 0; \\ \frac{N(N+1)}{4}, & \text{if } \ i = k = N; \\ 0, & \text{otherwise} \end{cases} \tag{15}$$

Now introduce

$$\bar{z}_k^N \quad = \quad z^N(\tau_k),\ k = 0, 1, \ldots, N$$

i.e. $\bar{z}_k^N$ is the value of polynomials $z^N(\tau)$ at LGL nodes τ_k. Throughout the paper, we use "bar" to denote the corresponding variable in the discrete space, and the superscript N to denote the variable depends on the number of nodes N. The subscript in $\bar{z}_k^N$ denotes the nodes τ_k. It is distinguished from the continuous-time case where the subscript in $z_i(t)$ is used to denote the i-th component of the state.

With these notations, the continuous differential equation can be approximated by the following nonlinear algebraic equations

$$\sum_{i=0}^{N} \bar{z}_i^N D_{ki} - \frac{\delta}{2} f(\bar{z}_k^N, \frac{\tau_k \delta - \delta + 2T}{2}) = 0,\ k = 0, \ldots, N \tag{16}$$

This discretization is used in [22, 2, 20] for optimal control problems. However, to guarantee feasibility of the discretization, the following relaxation proposed in [7, 6] is used

$$\left\| \sum_{i=0}^{N} \bar{z}_i^N D_{ki} - \frac{\delta}{2} f(\bar{z}_k^N, \frac{\tau_k \delta - \delta + 2T}{2}) \right\|_\infty \ \leq \ (N-1)^{\frac{3}{2} - m}, \qquad k = 0, 1, \ldots, N \tag{17}$$

When N tends to infinity, the difference between conditions (16) and (17) vanishes, since m, by assumption, is greater than or equal to 2. The reason for this specific type of relaxation is to guarantee the feasibility and the convergence of PS methods [7, 6]. As for the constraints, it can be discretized in a similar fashion

$$r(\bar{z}_k^N) \quad \leq \quad (N-1)^{\frac{3}{2} - m} \cdot \mathbf{1}, \quad k = 0, 1, \ldots, N \tag{18}$$

where $\mathbf{1}$ denotes $[1, \ldots, 1]^T$.

By the Gauss-Lobatto integration rule, the cost function $J(\cdot)$ can be approximated by

$$J[\hat{z}(\cdot)] \ \approx \ \bar{J}^N(\bar{z}_0^N, \ldots, \bar{z}_N^N) \quad = \quad \frac{\delta}{2} \sum_{k=0}^{N} \|\bar{z}_k^N - \bar{y}_k\|^2 w_k$$

where w_k are the LGL weights given by

$$w_k \quad = \quad \frac{2}{N(N+1)} \frac{1}{[L_N(\tau_k)]^2},$$

and

$$\bar{y}_k \quad = \quad y(\frac{\tau_k \delta - \delta + 2T}{2}), \qquad k = 0, 1, \ldots, N$$

are the output at the shifted LGL points. Hence, the optimization Problem 1 can be approximated by a nonlinear programming problem with $\bar{J}^N$ as the objective function and (17)—(18) as constraints.

Problem 2: Find $\bar{z}_k^N \in \mathbb{R}^{N_x}$, $k = 0, 1, \ldots, N$, that minimize

$$\bar{J}^N = \frac{\delta}{2} \sum_{k=0}^{N} \|\bar{z}_k^N - \bar{y}_k\|^2 w_k \tag{19}$$

subject to

$$\left\| \sum_{i=0}^{N} \bar{z}_i^N D_{ki} - \frac{\delta}{2} f(\bar{z}_k^N, \frac{\tau_k \delta - \delta + 2T}{2}) \right\|_\infty \leq (N-1)^{\frac{3}{2}-m}, \tag{20}$$

$$r(\bar{z}_k^N) \leq (N-r)^{\frac{3}{2}-m} \cdot \mathbf{1}, \tag{21}$$

for all $0 \leq k \leq N$.

2.2. **Feasibility and convergence.** The PS method for solving a continuous dynamic optimization problem consists of a specific discretization method that converts Problem 1 to a sequence of nonlinear programming problems, Problem 2. Then, well established optimization software can be applied to calculate the discrete-time optimal solution. Despite the simplicity of PS methods, there are some fundamental questions to be answered regarding the existence and convergence of a PS discretization of a continuous-time optimization problem. For instance, is the discretized optimization problem always feasible? If the discrete optimal solution is computed, does it converge to the continuous-time solution as N is increased? The answers to these fundamental questions are provided in this section. Most of the results in this section are adapted from [6, 7]. Interested readers are referred to [6, 7] for more inside.

Theorem 2.1. *Given any trajectory $x(t)$ satisfying Assumption 2, there exists a positive integer N_1 such that, for any $N > N_1$, the constraints (20)-(21) of Problem 2 has a feasible solution $\bar{z}_k^N$. Furthermore, the feasible solution satisfies*

$$\|\bar{x}_k - \bar{z}_k^N\|_\infty \leq L(N-1)^{1-m} \tag{22}$$

for all $k = 0, \ldots, N$, where $\bar{x}_k = x(\frac{\tau_k \delta - \delta + 2T}{2})$, τ_k are LGL nodes and L is a positive constant independent of N.

Proof. Let $\hat{x}(\tau)$ denote the trajectory $x(t)$ under transformation (9), i.e.,

$$\hat{x}(\tau) = x(\frac{\tau\delta - \delta + 2T}{2})$$

Based on Assumption 2 and Remark 2, $\hat{x}(\tau)$ is continuously differentiable and $\dot{\hat{x}}(\tau)$ has bounded $(m-1)$-th order distribution derivatives. Let $p(\tau)$ be the $(N-1)$-th order best approximation polynomial of $\dot{\hat{x}}(\tau)$ in the norm of $L^\infty(-1, 1)$. The following estimation has been proved in the literature of spectral methods (see [1])

$$\|\dot{\hat{x}}(\tau) - p(\tau)\|_{L^\infty} \leq C C_1 (N-1)^{1-m}, \quad \forall \tau \in [-1, 1] \tag{23}$$

where $C = \sum_{i=0}^{m-1} \|\dot{\hat{x}}^{(i)}\|_{L^\infty(-1,1)}$ and C_1 is a constant independent of N. Let us define

$$\hat{z}(\tau) = \int_{-1}^{\tau} p(s) ds + \hat{x}(-1)$$

From (23),

$$\|\hat{x}(\tau) - \hat{z}(\tau)\|_{L^\infty} \leq 2CC_1(N-1)^{1-m}, \quad \forall \tau \in [-1,1] \tag{24}$$

It follows that both $\hat{x}(\tau_k)$ and $\bar{z}_k^N$ are contained in some compact set whose boundary is independent of N. On this compact set, because $f(\cdot)$ is continuously differentiable, it must be Lipschitz continuous. In the following, we prove that $\bar{z}_k^N = \hat{z}(\tau_k)$ is a feasible solution of (20)-(21) satisfying (22).

By definition, $\hat{z}(\tau)$ is a polynomial of degree less than or equal to N. Given any polynomial of degree less than or equal to N, it is known (see [1]) that its derivative at the LGL nodes $\tau_0, \ldots, \tau_N$ are exactly equal to the value of the polynomial at the nodes multiplied by the differential matrix D, which is defined by (14)-(15). Thus we have $\sum_{i=0}^N \bar{z}_i^N D_{ki} = \dot{\hat{z}}(\tau_k)$ Therefore,

$$\begin{aligned}
&\left|\left|\sum_{i=0}^N \bar{z}_i^N D_{ki} - \frac{\delta}{2} f(\bar{z}_k^N, \frac{\tau_k\delta - \delta + 2T}{2})\right|\right|_\infty \\
&\leq \left|\left|\dot{\hat{z}}(\tau_k) - \dot{\hat{x}}(\tau_k)\right|\right|_\infty + \left|\left|\dot{\hat{x}}(\tau_k) - \frac{\delta}{2} f(\bar{z}_k^N, \frac{\tau_k\delta - \delta + 2T}{2})\right|\right|_\infty \\
&\leq \left|\left|p(\tau_k) - \dot{\hat{x}}(\tau_k)\right|\right|_\infty + \frac{\delta}{2}\left|\left|f(\hat{x}(\tau_k), \frac{\tau_k\delta - \delta + 2T}{2}) - f(\hat{z}(\tau_k), \frac{\tau_k\delta - \delta + 2T}{2})\right|\right|_\infty \\
&\leq CC_1(N-1)^{1-m} + \frac{\delta}{2} C_2 \|\hat{x}(\tau_k) - \hat{z}(\tau_k)\|_\infty \\
&\leq (CC_1 + \delta CC_1C_2)(N-1)^{1-m}
\end{aligned}$$

where C_2 is the Lipschitz constant of $f(\cdot)$. Since $m \geq 2$, there exists a positive integer N_1 such that, for all $N > N_1$,

$$(CC_1 + \delta CC_1C_2)(N-1)^{1-m} \quad \leq \quad (N-1)^{\frac{3}{2}-m}$$

Hence, (20) holds for all $N > N_1$.

As for the constraint (21), because $r(\cdot)$ is continuously differentiable, the following estimation holds.

$$\|r(\hat{x}(\tau)) - r(\hat{z}(\tau))\|_\infty \quad \leq \quad C_3\|\hat{x}(\tau) - \hat{z}(\tau)\|_\infty \ \leq \ 2CC_1C_3(N-1)^{1-m}$$

where C_3 is the Lipschitz constant of $r(\cdot)$ which is independent of N. Hence

$$r(\bar{z}_k^N) \quad \leq \quad r(\hat{x}(\tau_k)) + 2CC_1C_3(N-1)^{1-m} \cdot \mathbf{1} \ \leq \ 2CC_1C_3(N-1)^{1-m} \cdot \mathbf{1}$$

From here, constraint (21) holds for all $N > N_1$. Thus, we have constructed a feasible solution of (20)-(21) of Problem 2. As for (22), it follows directly from (24). □

Theorem 2.1 guarantees that Problem 2 is well-posed with a nonempty feasible set as long as a sufficient number of nodes is chosen. Therefore, an optimal solution always exists. More importantly, (22) shows the existence of a feasible discrete solution around any neighborhood of the continuous trajectory. With this existence result in hand, we can further explore convergence properties. The convergence results are derived in a way similar to Polak's Consistent Approximation [17]. Let $(\bar{z}_0^{*N}, \ldots, \bar{z}_N^{*N})$ be an optimal solution to Problem 2, and $z^N(\tau) \in \mathbb{R}^{N_x}$ be the N-th order interpolating polynomial of $(\bar{z}_0^{*N}, \ldots, \bar{z}_N^{*N})$, i.e.

$$z^N(\tau) \quad = \quad \sum_{k=0}^N \bar{z}_k^{*N} \phi_k(\tau) \tag{25}$$

where $\phi_k(\tau)$ is defined by (13).

Assumption 3. It is assumed that the sequences $\left\{\bar{z}_0^{*N}\right\}_{N=N_1}^{\infty}$ converges as $N \to \infty$. Furthermore, there exists a continuous function $q(\tau) \in \mathbb{R}^{N_x}$ such that $\dot{z}^N(t)$ converges to $q(\tau)$ uniformly on $\tau \in [-1, 1]$.

Theorem 2.2. *Let $\{\bar{z}_0^{*N}, \ldots, \bar{z}_N^{*N}\}_{N=N_1}^{\infty}$ be a sequence of discrete optimal solutions of Problem 2. Assume the sequence satisfies Assumption 3, then the following limits converge uniformly*

$$\lim_{N\to\infty} \bar{J}^N(\bar{z}_0^{*N}, \ldots, \bar{z}_N^{*N}) = 0 \tag{26}$$

$$\lim_{N\to\infty} (\bar{z}_k^{*N} - \bar{x}_k) = 0 \tag{27}$$

for all $0 \le k \le N$, where $\bar{x}_k = x(\frac{\tau_k\delta - \delta + 2T}{2})$ and τ_k are LGL nodes.

Before the proof of Theorem 2.2, we must introduce the following lemmas.

Lemma 2.3. [3] *Let τ_k, $k = 0, 1, \ldots, N$, be LGL nodes, w_k be LGL weights. Suppose $\phi(\tau)$ is Riemann integrable, then $\int_{-1}^{1} \phi(\tau)d\tau = \lim_{N\to\infty} \sum_{k=0}^{N} \phi(t_k)w_k$.*

Lemma 2.4. *Let τ_k, $k = 0, 1, \ldots, N$, be LGL nodes. Suppose that $z(t)$ is continuous on $[T - \delta, T]$. Assume*

$$\lim_{N\to\infty} (\bar{z}_k^N - z(\frac{\tau_k\delta - \delta + 2T}{2})) = 0 \tag{28}$$

uniformly in k, then we have

$$\lim_{N\to\infty} \bar{J}^N(\bar{z}_0^N, \ldots, \bar{z}_N^N) = J[z(\cdot)] \tag{29}$$

where $\bar{J}^N$ and J are the cost functions defined by (5) and (19), respectively.

Proof. Transfer the time domain from $[T-\delta, T]$ to $[-1, 1]$ and denote $\tau = \frac{2t-2T+\delta}{\delta}$

$$\hat{z}(\tau) = z(\frac{\tau\delta - \delta + 2T}{2})$$

$$F(\hat{z}(\tau), \tau) = \|h(\hat{z}(\tau)) - y(\frac{\tau\delta - \delta + 2T}{2})\|^2$$

From the uniform convergence property of $\bar{z}_k^N$, it is easy to conclude $\bar{z}_k^N$ is bounded for all $N \ge 1$ and $0 \le k \le N$. Therefore,

$$|F(\hat{z}(\tau_k), \tau_k) - F(\bar{z}_k^N, \tau_k)| \le K|\hat{z}(\tau_k) - \bar{z}_k^N| \tag{30}$$

for some $K > 0$ and for all $N \ge 1$, $0 \le k \le N$. Apparently, $F(\hat{z}(\tau), \tau)$ is continuous in τ; hence it is Riemann integrable. Applying Lemma 2.3, we have

$$\int_{-1}^{1} F(\hat{z}(\tau), \tau)d\tau = \lim_{N\to\infty} \sum_{k=0}^{N} F(\hat{z}(\tau_k), \tau_k)w_k$$

Therefore,

$$\int_{-1}^{1} F(\hat{z}(\tau), \tau)d\tau = \lim_{N\to\infty} \left(\sum_{k=0}^{N} F(\bar{z}_k^N, \tau_k)w_k + \sum_{k=0}^{N} \left(F(\hat{z}(\tau_k), \tau_k) - F(\bar{z}_k^N, \tau_k)\right) w_k \right)$$

From the uniform convergence of (28) and the property of w_k, $\sum_{k=0}^{N} w_k = 2$, we know that

$$\lim_{N\to\infty} \sum_{k=0}^{N} \left(F(\hat{z}(\tau_k),\tau_k) - F(\bar{z}_k^N,\tau_k)\right) w_k \leq \lim_{N\to\infty} K \sum_{k=0}^{N} \left(|\hat{z}(\tau_k) - \bar{z}_k^N|\right) w_k \;=\; 0$$

Thus,

$$\int_{-1}^{1} F(\hat{z}(\tau),\tau)d\tau \quad = \quad \lim_{N\to\infty} \sum_{k=0}^{N} F(\bar{z}_k^N,\tau_k) w_k$$

It follows that

$$\begin{aligned}
\lim_{N\to\infty} \bar{J}^N(\bar{z}_0^N,\ldots,\bar{z}_N^N) &= \frac{\delta}{2} \lim_{N\to\infty} \sum_{k=0}^{N} F(\bar{z}_k^N,\tau_k) w_k \\
&= \frac{\delta}{2} \int_{-1}^{1} F(\hat{z}(\tau),\tau)d\tau \\
&= \int_{T-\delta}^{T} \|h(z(t)) - y(t)\|^2 dt \\
&= J[z(\cdot)]
\end{aligned}$$

□

Proof of Theorem 2.2: Based on Assumption 3, let z_0^∞ be the limit of $\left\{\bar{z}_0^{*N}\right\}_{N=N_1}^{\infty}$. Then, define the following functions

$$\eta(\tau) \quad = \quad \int_{-1}^{\tau} q(\tau)d\tau + z_0^\infty$$

In the following we will show that $\eta(\tau)$ satisfies the differential equation (10) and the constraint (11). By Assumption 3 and the definition of $z^N(\tau)$, the uniformly convergence property of $\dot{z}^N(\tau)$ implies

$$\lim_{N\to\infty} z^N(\tau) = \int_{-1}^{\tau} \lim_{N\to\infty} \dot{z}^N(\tau)d\tau + \lim_{N\to\infty} z^N(-1) = \eta(\tau) \tag{31}$$

Moreover the convergence is uniformly in τ.

Define

$$e(\tau) \quad = \quad \dot{\eta}(\tau) - \frac{\delta}{2} f(\eta(\tau), \frac{\tau\delta - \delta + 2T}{2})$$

Using contradiction argument, suppose $\eta(\tau)$ is not the solution of the differential equation (10). Then there is a time instance $\tau' \in [-1,1]$ so that

$$e(\tau') \quad = \quad \dot{\eta}(\tau') - \frac{\delta}{2} f(\eta(\tau'), \frac{\tau'\delta - \delta + 2T}{2}) \neq 0 \tag{32}$$

Because the nodes τ_k are getting dense as N tends to infinity [3], there exists a sequence i^N satisfying

$$0 \leq i^N \leq N \qquad \text{and} \qquad \lim_{N\to\infty} \tau_{i^N} = \tau'$$

Since $z^N(\tau)$ and $\dot{z}^N(\tau)$ converge uniformly, we have

$$e(\tau') \quad = \quad \lim_{N\to\infty} e(\tau_{i^N}) \;=\; \lim_{N\to\infty} (\dot{z}^N(\tau_{i^N}) - \frac{\delta}{2} f(z^N(\tau_{i^N}), \frac{\tau_{i^N}\delta - \delta + 2T}{2}))$$

Because $z^N(\tau)$ is the interpolating polynomial and $z^N(\tau_{i^N})$ satisfies (17), the following equation holds

$$\begin{aligned} e(\tau') &= \lim_{N\to\infty}(\dot{z}^N(\tau_{i^N}) - \frac{\delta}{2}f(z^N(\tau_{i^N}), \frac{\tau_{i^N}\delta - \delta + 2T}{2})) \\ &= \lim_{N\to\infty}(N-1)^{\frac{3}{2}-m} = 0 \end{aligned}$$

It contradicts to (32). Therefore, $\eta(\tau)$ must be a solution of differential equation (10). The constraint (11) can be proved by the same contradiction argument. Now define

$$z^\infty(t) = \eta(\frac{2t - 2T + \delta}{\delta}).$$

It is easy to show $z^\infty(t)$ is a feasible solution to Problem 1. Moreover, by (31)

$$\lim_{N\to\infty}(\bar{z}_k^{*N} - z^\infty(\frac{\tau_k\delta - \delta + 2T}{2})) = 0 \tag{33}$$

uniformly for $0 \le k \le N$. In the next, we prove that $z^\infty(t)$ is indeed the optimal solution of the continuous Problem 1. According to Theorem 2.1, there exists a sequence of feasible solutions, $\tilde{z}_k^N$, of discrete Problem 2 that uniformly converges to the trajectory $x(t)$. Now, from Lemma 2.4 and the optimality of $x(t)$ and $\bar{z}_k^{*N}$, we have

$$\begin{aligned} 0 &\le J[z^\infty(\cdot)] = \lim_{N\to\infty}\bar{J}^N(\bar{z}_0^{*N}, \ldots, \bar{z}_N^{*N}) \\ &\le \lim_{N\to\infty}\bar{J}^N(\tilde{z}_0^N, \ldots, \tilde{z}_N^N) \\ &= J[x(\cdot)] = 0 \end{aligned}$$

Therefore, (26) holds. Above argument shows that $z^\infty(t)$, a feasible solution to continuous Problem 1, achieves optimal cost which is 0. Therefore, $z^\infty(t)$ is an optimal solution to the continuous Problem 1. Since Problem 1 has an unique optimal solution $x(t)$, $z^\infty(t)$ must be identical to the unmeasurable state trajectory $x(t)$. Hence, (27) follows (33). □

3. **Pseudospectral observer.** In this section, we show how to construct a PS observer based on a moving horizon strategy. The main observer algorithm is presented in Section 3.1. The fast convergence property of the purposed observer algorithm is addressed in Section 3.2. The observer tuning parameters are analyzed in Section 3.3. The performance of the proposed observer under measurement noise is presented in Section 3.4. Finally a DAE example is given in Subsection 3.5. Throughout this section, a family of chaotic Duffing systems is used to illustrate the key properties.

3.1. **Observer algorithm.** Let $\{t_i\}_{i=0}^\infty$ be the sequence of sampling time with $\lim_{i\to\infty} t_i = \infty$. Denote $y_i = y(t_i)$, i.e., y_i is the measurement of the output $y(t)$ at the sample point t_i. The observer problem is to estimate the state $x(t)$ at the current sampling time t_p based on the measurement $\{y_i\}_{i=0}^p$ and the system model. By the moving horizon strategy, during each sampling period the continuous-time optimization Problem 1 is solved online by the PS method. Then the estimation of the current state is given by the optimal solution of the discrete Problem 2. A pseudospectral observer is formulated as the following algorithm.

Initialization:

1. Select tuning parameters N, L and initial guess of $x(t_0)$, where $N > 1$ and $L > 1$ are positive integers, N represents the number of nodes used in the pseudospectral discretization and L represents the number of data to be processed at each iteration. If the sampling period is ΔT, then the backward integration length is $\delta = \Delta T \cdot L$.
2. Calculate the LGL nodes τ_k, LGL weights w_k, $k = 0, 1, \ldots, N$, and the differential matrix D.
3. Propagate the initial guess of $x(t_0)$ by the differential equation (1) to generate the guess of the state at the shifted LGL notes $\frac{(\tau_k+1)(t_L-t_0)+2t_0}{2}$. Denote the guess as $\hat{z}_k^-$, $0 \le k \le N$, where the superscript "$-$" means prediction or a priori estimation. Set $Z_{initial} = \{\hat{z}_k^-\}_{k=0}^N$. Here $Z_{initial}$ is the starting point/initial guess for the optimization software. It is different from the initial guess of $x(t_0)$.
4. Collect initial data $\{y_0, y_1, \ldots, y_{L-1}\}$ and set $p = L$.

Main algorithm:

1. Collect the new measurement y_p.
2. Construct the spline function $y^s(t)$ of the data $\{y_{p-L}, y_{p-L+1}, \ldots, y_p\}$ such that $y^s(t_i) = y_i$ for all $p - L \le i \le p$. Set $\bar{y}_k = y^s(\frac{\tau_k\delta-\delta+2T}{2})$, where $\delta = t_p - t_{p-L}$ and $k = 0, 1, \ldots, N$. Here $\bar{y}_k$ is the reference signal in the cost function of Problem 2.
3. Apply nonlinear programming solver to Problem 2 with initial guess as $Z_{initial}$ to get the optimal solution $\{\bar{z}_k^{*N}\}_{k=0}^N$. The estimation of the current state $x(t_p)$ is given by $\bar{z}_N^{*N}$.
4. Propagate $\bar{z}_N^{*N}$ to the differential equation (1) to get the prediction of the state at the next sampling time t_{p+1}. Denote the prediction as $\hat{x}_{p+1}^-$.
5. Construct the spline function $\hat{z}^s(t)$ of the data $\{\bar{z}_0^{*N}, \ldots, \bar{z}_N^{*N}, \hat{x}_{p+1}^-\}$.
6. Set $p = p + 1$ and $Z_{initial} = \{\hat{z}^s(\frac{\tau_k\delta-\delta+2T}{2})\}_{i=0}^N$.
7. Go to step 1.

Remark 3. For the reason of simplicity, we fix the parameters N and L to be constants for each iteration. In general, they can be changed at any sampled instance. For example, in the beginning, L can be chosen as a small integer. As more and more measurements become available, L can be set to a relatively large number to incorporate more data.

Remark 4. The pseudospectral discretization of Problem 1 requires the measurement $y(t)$ at shifted LGL nodes, i.e., $y(\frac{\tau_k\delta-\delta+2T}{2})$. But in practice, the sampling time does not coincide with the nodes. To overcome this difficulty, spline function $y^s(t)$ is introduced in Step 2 of the main algorithm. If the sampling rate is sufficiently fast, the difference between $y^s(t)$ and the true output $y(t)$ is very small. Therefore, by the convergence results presented in the previous section, the optimal solution $\bar{z}_N^{*N}$ is also close to $x(t_p)$ if the number of LGL nodes is sufficiently large.

Remark 5. The proposed observer algorithm is a prediction-correction scheme. After Step 3 of the main algorithm, the current estimation $\bar{z}_N^{*N}$ is used to generate a good prediction of the state at the next sampling time t_{p+1} by some numerical integration algorithm like a Runge-Kutta method. Then, this prediction is used to form an initial guess for the optimization solver in the next iteration. The optimization performed in Step 3 of the main algorithm acts as a correction to the

prediction provided by numerical integration. This prediction-correction scheme greatly reduces the running time, because the optimization at step $p+1$ only needs to be done locally in a small neighborhood around the initial guess.

Clearly, the main computational burden in the proposed observer algorithm is in Step 3, where a nonlinear programming needs to be solved. To successfully apply the algorithm, the optimal solution of Problem 1 needs to be calculated in a time period much shorter than the sampling period $\Delta T = t_{p+1} - t_p$. The nature of pseudospectral discretization makes this possible. When PS methods are used to approximate a smooth function, the convergence is at a spectral rate [1]. It implies that only a small number of nodes are needed to get accurate approximation. As far as optimization is concerned, reducing the number of nodes means the number of decision variables and constraints are also reduced, which in turn decreases the running time for solving Problem 2 up to a point. There are other possible techniques to increase the computational speed for PS methods. For example:

- At each iteration, after solving the optimization problem, the covector mapping theorem [6, 7] can be used to warm-start the nonlinear programming solver in the next run. It significantly reduces the computational load for SQP-based nonlinear programming methods that utilize an active-set strategy.
- Problem 2 does not need to be solved at every iteration. Since the optimal cost of Problem 1 is always zero, we can use it as an error estimator. If the cost based on the prediction is very small, we can simply take the prediction as our estimation. Then, until the cost is larger than some threshold value, no optimization needs to be performed.
- The running time for solving Problem 2 can be reduced by using faster computers and/or software intended for real-time applications. It is also possible to use hardware technology like Application-Specific Integrated Circuits (ASIC) or Field Programmable Gate Arrays (FPGA) to achieve fast running time.

Although none of these ideas were used in this paper, they are delineated to simply note that computational speeds far greater than that reported in this section are quite possible.

To demonstrate the efficiency of the proposed observer algorithm, we present an observer design for a forced Duffing system. We choose this system because it is a nonlinear, time-varying, chaotic system with an unknown parameter. Even worse, the system is not uniformly observable, which renders many gain-based methods inapplicable.

Example 1.

$$\begin{aligned} \dot{x}_1 &= x_2 \\ \dot{x}_2 &= -0.25x_2 + x_1(1 - x_1^2) + \theta\cos(t) \\ y &= x_1 + 0.5x_2 \end{aligned} \tag{34}$$

where θ is an unknown parameter. In the simulations θ is set to be 0.4. This choice of parameter makes the performance of the system chaotic. The sampling time is $t_p = 0.1p$, $p = 0, 1, 2, \cdots$, and the measured output is $y_p = y(t_p)$. The observer design for system (34) is difficult, since it is a time-varying chaotic system with uncertainty [10].

By treating θ as an extra state with the dynamic $\dot{\theta} = 0$, we apply the proposed pseudospectral algorithm to construct an observer. In the simulation, we choose

the initial condition of (34) to be $(x_1(0), x_2(0)) = (2, 1)$ which is unknown to the observer. The tuning parameters are set to $N = 15$, $L = 8$ and the guess of the initial condition is $(0, 0)$. All simulations presented in this paper are programmed in MATLAB on a Pentium 4, 2.4GHz PC with 256MB of RAM. The spline function in the main algorithm is constructed using cubic spline interpolation provided by MATLAB. The overall computation is carried out by using DIDO, a software of optimal control using the Legendre PS method.

The results are demonstrated in Figure 1. Once the initial data $(y_0, \ldots, y_L)$ are collected, the PS observer provides accurate estimation of both the state and the unknown parameter. Actually, the estimation errors of x_1 and x_2 are within 10^{-4} while the error in θ is less than 10^{-3}. The average running time for each iteration is about 0.05 second.

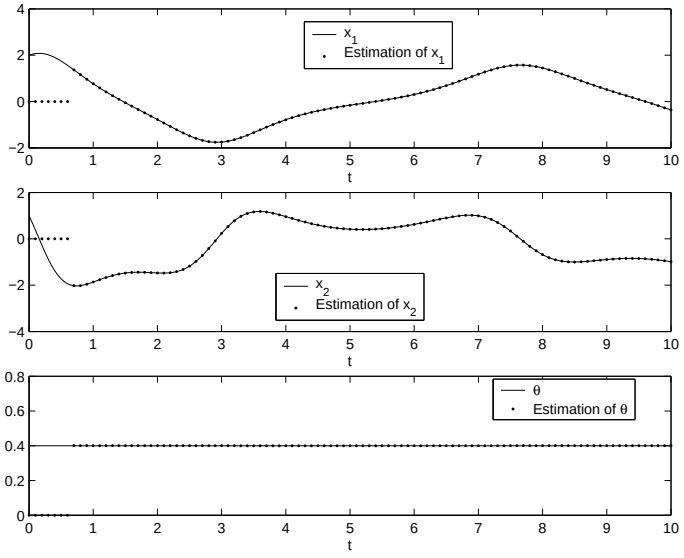

FIGURE 1. PS observer for a Duffing system with uncertainty.

3.2. **Convergence property.** In many observer design methods such as the Extended Kalman Filter, the Unscented Kalman filter, the High-gain observer and some moving horizon observers, the convergence of the estimation error is asymptotic. This means it takes certain period of time for the estimated state to be close to the true state trajectory and the convergence time depends on the system and the observer parameters. In the proposed pseudospectral observer algorithm, the convergence of the estimated state is very fast. As clearly demonstrated in Example 1, in the first step of the iteration at t_{L-1}, the error is already close to zero. It takes virtually no time for convergence once the algorithm is started. The reason for this impressive property is very simple. In Problem 1, the unique optimal solution is the unmeasured state, $x(t)$. Hence, from the convergence property presented in the previous section, at each iteration, if an optimal solution of Problem 2 is found, it must lie in an ϵ-neighborhood of $x(t)$.

The fast convergence property of the proposed algorithm is very attractive in practice, especially in the design of output feedback controllers. It qualifies the

proposed PS observer as a numerical sensor which can be embedded in the control system to construct an output feedback controller [8]. In what follows, we use an example to show that the finite-time convergence property is also important to guarantee the stability of the observer.

Example 2. Consider a modification to the Duffing system in Example 1. Let θ be given by

$$\theta \quad = \quad \begin{cases} 0.4; & t \leq 10 \\ 0.1; & 10 < t \leq 20 \\ 0.3; & 20 < t \end{cases}$$

The sampling rate and the tuning parameters are the same as Example 1. In Figure 2(a,b,c), the estimation error of the state (x_1, x_2) and the estimated unknown parameter are plotted. Obviously, the jumps in θ create no difficulty for the PS observer because of its fast convergence rate. As a comparison, the performance of an Unscented Kalman Filter [9] (UKF) is also presented in Figure 2 (d,e,f). The tuning parameters of UKF are chosen such that it converges for a fixed θ (without jumps). In contrast to the PS observer, the sluggish convergence of the unknown parameter destroys the convergence of the state estimation.

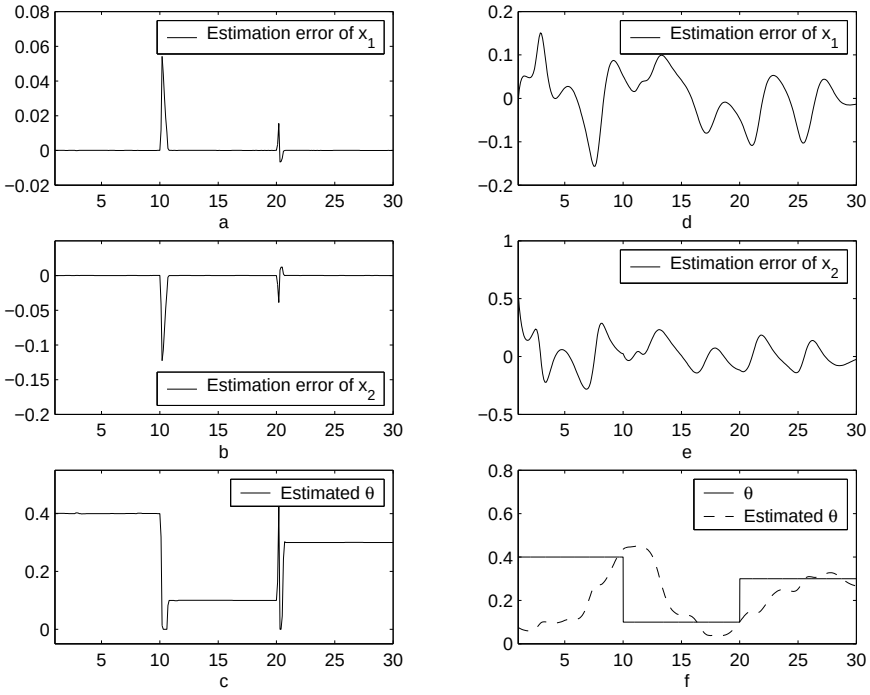

FIGURE 2. Performance of PS observer and UKF for Duffing system with jump uncertainty. Figure a, b, and c are results from a PS observer, with tuning parameter $L = 8$, $N = 15$ and initial guess $(0, 0, 0.1)$. Figure d, e, and f are results from a UKF, with the same initial guess as the PS observer.

3.3. **Tuning parameters.** In the pseudospectral observer, there are three tuning parameters: 1) the backward integration length L; 2) the number of the discretization nodes N; and 3) the initial guess of the state $x(0)$. In this subsection we briefly discuss these tuning parameters.

Theoretically speaking, Assumption 1 guarantees that L can be any positive integer. However, in practice we want to set L as large as possible within the limit of real-time computation, because a larger value of L implies a more accurate estimation. However, increasing L results in the increase of the integration length in the cost function of Problem 1. Correspondingly, a larger number of nodes N are needed in order to get an accurate discretization of the continuous optimization Problem 1. Thus the trade off for L is in the computational time versus the accuracy. Compared with other discretization methods, like Euler and Runge-Kutta, pseudospectral methods normally require much smaller N to achieve the same level of accuracy when a nonlinear function is approximated. Therefore, for the same number of nodes, a pseudospectral observer can deal with much longer integration lengths than other discretization schemes.

Another factor that influences the performance of the observer is the relationship between the pair, (L, N) and the sampling frequency. In order for the observer to work for different sampling frequencies, we recommend the following general rule: the smaller the sampling period, the larger the L can be. So if the sampling period is decreased by ten times, we can enlarge L by a factor of ten and keep the same number of discretization nodes N, because the integration length remains the same in these two situations. In the following example we show how to choose appropriate tuning parameter L and N according to different sampling frequencies.

Example 3. Consider again the observer design for the uncertain Duffing system (34). We now choose the sampling period to be 0.01. Accordingly, we choose L to be 80, ten times the value chosen in Example 1, while keeping the number of nodes to be the same as before. The observer performance with this choice of parameters is shown in Figure 3(a,b,c). Also shown in Figure 3(d,e,f) is the performance when the sampling period is 0.5 and the tuning parameters are set to $L = 10$ and $N = 50$. It is clear that in both situations, the performance of the observer is very good.

The guess of the initial condition for the PS observer is not a key factor. Unlike the Extended Kalman Filter or other local observer design methods where a bad choice of the initial guess will lead to an unstable observer, our observer is not sensitive to the initial condition. The attractive region depends only on the convergence region of the optimization solver. Since many good nonlinear programming methods are globally convergent under mild assumptions, robustness of the PS observer is essentially assured.

3.4. **Measurement noise.** In this section, we assume that the measurement is corrupted by a noisy signal. This situation is quite common in practice and must be carefully addressed in order to apply the observer to real systems. In this section, we first show how well the PS observer works under measurement noise. Then, we discuss some possible ways to improve the performance.

A first rule to deal with the measurement noise is to increase the integration length. In other words, we can set a large number for L so that more information is used by the observer. In addition, we will develop in this section a new method using the constrained optimization method to further reduce the impact of the noise. In the following, we use an example to demonstrate the points.

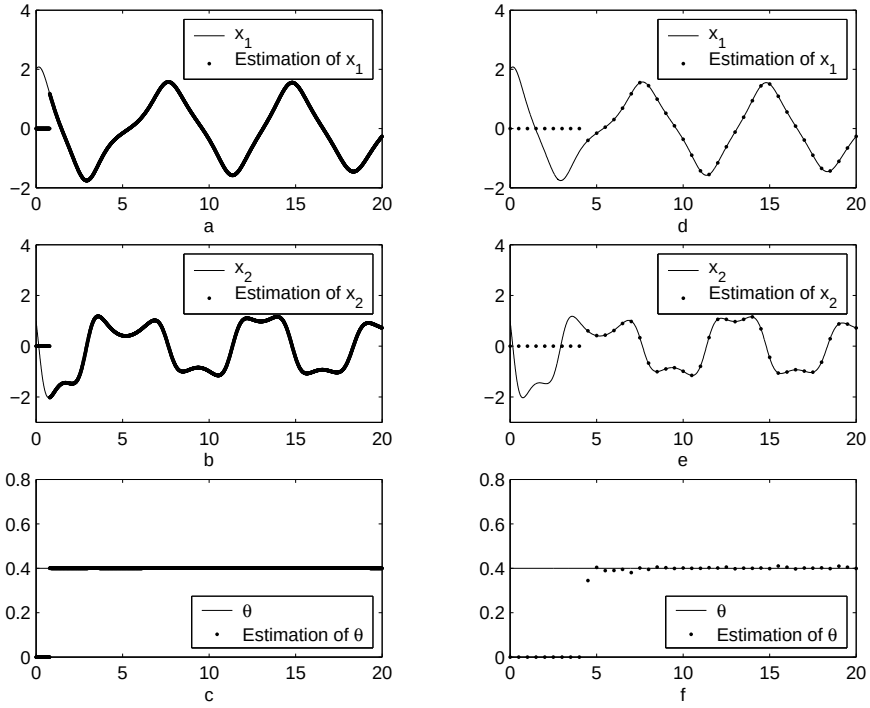

FIGURE 3. PS observer for a Duffing system with different sampling frequencies. In figure a, b, and c the sampling period is 0.01 and the tuning parameters are chosen as $L = 80$, $N = 15$. In figure d, e, and f the sampling period is 0.5 and $L = 10$, $N = 50$.

Example 4. Consider the Duffing system with noisy measurements:

$$\begin{aligned} \dot{x}_1 &= x_2 \\ \dot{x}_2 &= -0.25x_2 + x_1(1 - x_1^2) + 0.4\cos(t) \\ y &= x_1 + 0.5x_2 + d(t) \end{aligned} \tag{35}$$

where $d(t)$ represents the unknown disturbance. In the simulation we choose $d(t)$ to be a uniformly distributed random signal in the interval $[-1, 1]$. The sampling period is 0.1 and the initial condition is $(x_1(0), x_2(0)) = (1, 2)$. The parameters of the observer are chosen as $L = 50$, $N = 50$ and the initial guess is $(0, 0)$. Note that as a result of the measurement noise, L is chosen to be much larger than the one used in Example 1. The performance of the proposed observer is presented in Figure 4. It is clear that the estimation errors of the output are less than one half of the measurement noise.

The noise can be further reduced by utilizing the constrained optimization technique. In the following, we modify the PS observer algorithm to incorporate disturbance information into the numerical observer. Assume the system to be observed is

$$\begin{aligned} \dot{x} &= f(x(t), t) \\ y_i &= h(x(t_i)) + d_i \end{aligned}$$

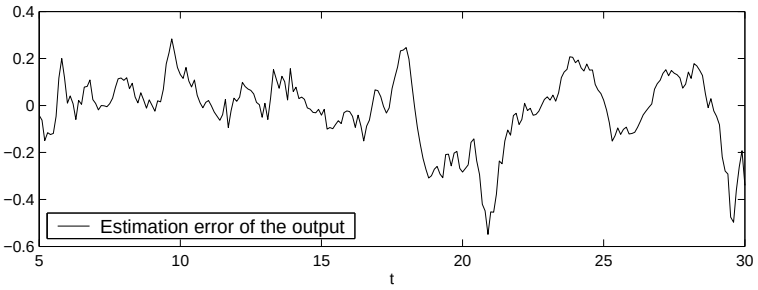

FIGURE 4. Performance of a PS observer for a Duffing system with measurement noise.

where d_i is a bounded disturbance/noise with a known bound, b, i.e.,

$$\|d_i\| \quad \leq \quad b$$

Our modification includes two part. Firstly, the bounded disturbance is modelled in Problem 1 as a constraint. Specifically, the new definition of Problem 1 is:

Problem 1: Determine the function $z(t)$, that minimizes the cost function

$$J[z(\cdot)] \quad = \quad \int_{T-\delta}^{T} \|h(z(t)) - y(t)\|^2 dt \tag{36}$$

subject to the state equation

$$\dot{z}(t) \quad = \quad f(z(t), t) \tag{37}$$

and constraint

$$\sigma_1(y_i, b) \ \leq \ h(z(t_i)) \quad \leq \quad \sigma_2(y_i, b) \tag{38}$$

where $\sigma_1(\cdot)$ and $\sigma_2(\cdot)$ represent upper and lower bound of the estimated output.

One apparent choice for $\sigma_1(\cdot)$ and $\sigma_2(\cdot)$ is

$$\sigma_1(y_i, b) = y_i - b \ \text{ and } \ \sigma_2(y_i, b) = y_i + b \tag{39}$$

It specifies a tube based on the measurement and the bound of the disturbance, in which the estimated output must lie. Formula (39) is easy to implement; however it is not necessarily the best choice for the bounding functions $\sigma_1(\cdot)$ and $\sigma_2(\cdot)$. Indeed, as the estimation window moving along the time horizon and the new measurements been collected, the bound of the estimated output can be made much tighter. The idea can be explained in the following plot. At each sampling instance T, after solving Problem 1, the current estimation of the output and also the prediction of the output at the next sampling instance can be calculated; see step 3 and 4 of the main algorithm. Denote the predicted output as y_{pre}. Since on the time interval $t \in [T-\delta, T]$, the "clean" output and the estimated output all lie in the tube bounded by σ_1 and σ_2, y_{pre} and the "clean" output at $T + \Delta T$ should also be bounded. Based on the past data on the interval $[T-\delta, T]$, the possible region of the output at the next sampling instance can be determined. Intuitively, this feasible region based on past date can be gotten by propagating every solution that lies in the tube on the time interval $[T-\delta, T]$ to the next sampling instance $T + \Delta T$. In Figure 5, this possible region is demonstrated. When the new output, $y(T + \Delta T)$, is measured, based on the disturbance bound, we can get another possible region

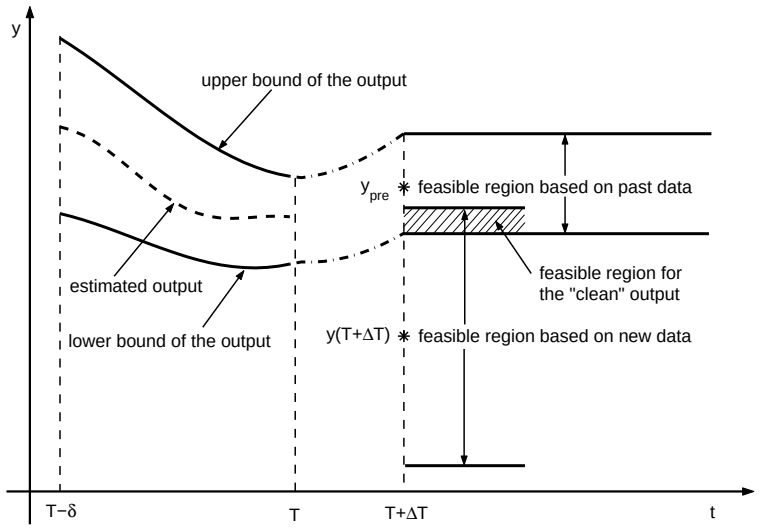

FIGURE 5. Refinement of the constraint set. T is the current time; ΔT is the sampling interval; and δ is the backward integration length. y_{pre} represents the prediction of the output based on past data; and $y(T+\Delta T)$ is the measured output at $T+\Delta T$.

for the "clean" output. Apparently, the intersection of these two regions lies the real output $h(x(T+\Delta T))$; and the bound of this intersected area forms the upper and lower bounds, $\sigma_1(\cdot)$, $\sigma_2(\cdot)$, at the new sampling instance.

To calculate the feasible region based on the past data, we formulate the following optimization problem after step 4 of the main algorithm when the prediction y_{pre} is available.

Problem 3: Determine the function $z(t)$, that *maximizes* the cost function

$$J[z(\cdot)] \quad = \quad \|h(z(T+\Delta T)) - y_{pre}\|^2$$

subject to the state equation

$$\dot{z}(t) \quad = \quad f(z(t),t), \qquad t \in [T-\delta, T+\Delta T]$$

and constraint

$$\sigma_1(y_i,b) \;\leq\; h(z(t_i)) \quad \leq \quad \sigma_2(y_i,b), \quad \forall t_i \in [T-\delta, T]$$

The optimal solution of Problem 3 defines the feasible region based on past data. Actually, at the next sampling instance $T+\Delta T$, the estimation must satisfy

$$y_{pre} - \sqrt{J^*} \;\leq\; h(z(T+\Delta T)) \quad \leq \quad y_{pre} + \sqrt{J^*} \tag{40}$$

where J^* is the optimal value function of Problem 3. From the definition of Problem 3, it is easy to show that the feasible region based on past data, i.e., (40), must have an intersection with the feasible region based on the new measurement. And the bounds of the output at $t = T+\Delta T$ are given by

$$\begin{aligned} \sigma_1 &= \max\{y_{pre} - \sqrt{J^*}, y(T+\Delta T) - b\} \\ \sigma_2 &= \min\{y_{pre} + \sqrt{J^*}, y(T+\Delta T) + b\}. \end{aligned}$$

The same procedure is repeated as the estimation windows moving forward.

Now applying this new PS observer algorithm, we resolved Example 4 with the same tuning parameters. The results are shown in the following figure. Compared to

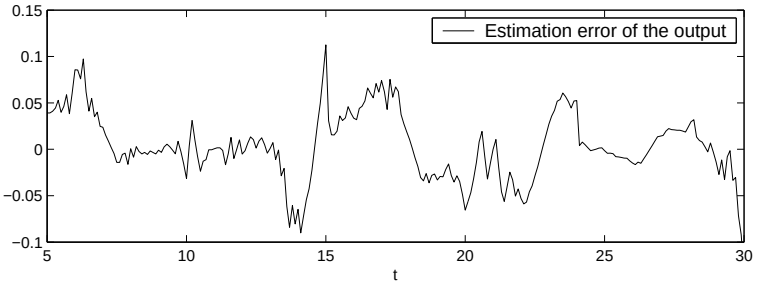

FIGURE 6. Performance of a PS observer for a Duffing system with measurement noise.

Figure 4, the impact of the noise is further reduced. Actually, since the measurement noise belongs to $[-1, 1]$, Figure 6 shows a reduction of the noise by 90%.

Remark 6. In the modified observer algorithm, at every iteration, two optimization problems need to be solved. Solution to Problem 3 provides the bounding information of the estimated output and Problem 1 gives the estimated states. The combination of the two problems greatly reduces the estimation error at the price of more computational burden. However, the running time of each iteration does not increase too much. For instance, the average running time in Example 4 is about 0.5 second; while the average running time with the modified algorithm is about 0.7 second. The reason is that, the solution to Problem 3 provides a tight bound. Therefore, the search region for Problem 1 is greatly reduced.

Example 5. Consider the Duffing system with measurement noise,

$$\begin{aligned} \dot{x}_1 &= x_2 \\ \dot{x}_2 &= -0.25x_2 + x_1(1 - x_1^2) + \theta\cos(t) \\ y &= x_1 + 0.5x_2 + d(t) \end{aligned}$$

and jump unknown parameter

$$\theta = \begin{cases} 0.4; & t \leq 15 \\ 0.1; & 15 < t \leq 35 \\ 0.6; & 35 < t \end{cases}$$

The measurement noise is assumed to be uniformly distributed random signal in the interval $[-0.1, 0.1]$.

The sampling rate is 0.1 and the tuning parameters are chosen as $L = 50$, $N = 50$. We test the algorithm for 100 runs under randomly selected initial condition on $(x_1(0), x_2(0)) \in [-1, 1]$. The average root mean square error of the states and the average estimation of the unknown parameter are shown in the Figure 7. Apparently, the estimation for the state and the unknown parameter are quite accurate even with the appearance of the measurement noise and jump uncertainty. It is interesting to known that for this example, Unscented Kalman Filter fails to converge even after a carefully tuning of the filter parameters.

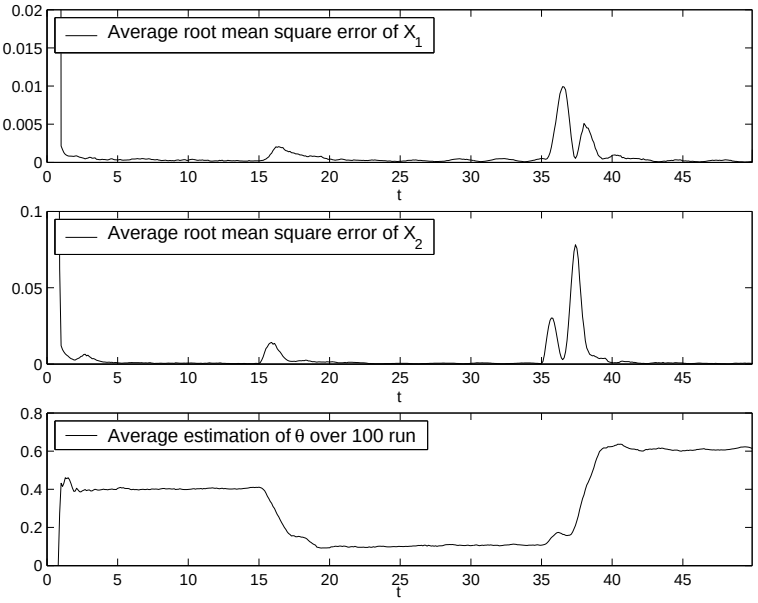

FIGURE 7. The average root mean square error of the states and the average estimation of the unknown parameter over 100 random runs.

3.5. **A DAE example.** The observer design for nonlinear systems governed by deferential-algebraic equations is a very challenge problem. Many gain-based observer design methods are not applicable to DAE systems, since they are fundamentally based on ODEs. For our PS numerical observer, the algebraic equations can be modeled by the constraint set. Therefore, the estimation of the unobserved states is still possible by the proposed online optimization framework. In this section, we use a nonlinear circuit example from [19] to demonstrate the validity of the PS observer for DAE systems.

Example 6. Consider the RLC circuit displayed in Figure 8, where R is a linear resistor, L is a linear inductor and C is a nonlinear capacitor. The systems is governed by the DAE:

$$\begin{aligned} \dot{x}_1 &= x_2/L \\ \dot{x}_2 &= -x_2R/L - x_3 + 1 \\ 0 &= -x_1 + (x_3-1)^3 - (x_3-1) + 1 \\ y &= x_2 \end{aligned} \tag{41}$$

where x_1 is the charge in the nonlinear capacitor, x_2 is the magnetic flux in the inductor and x_3 is the voltage on the capacitor. Due to the nonlinear charge-voltage character of the capacitor, the circuit has singularity-induced bifurcation [19] which makes the estimation of the unobservable state very difficult. Nevertheless, from the simulation results in Figure 9, the PS observer still works for DAE system (41).

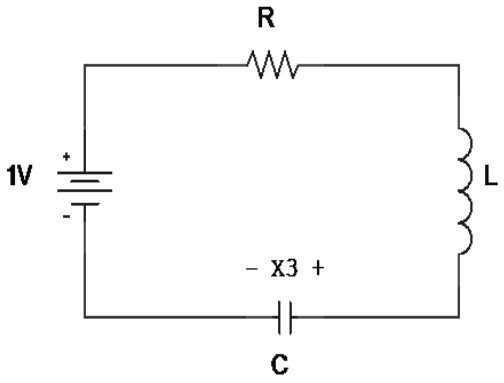

FIGURE 8. Nonlinear RLC circuit from [19].

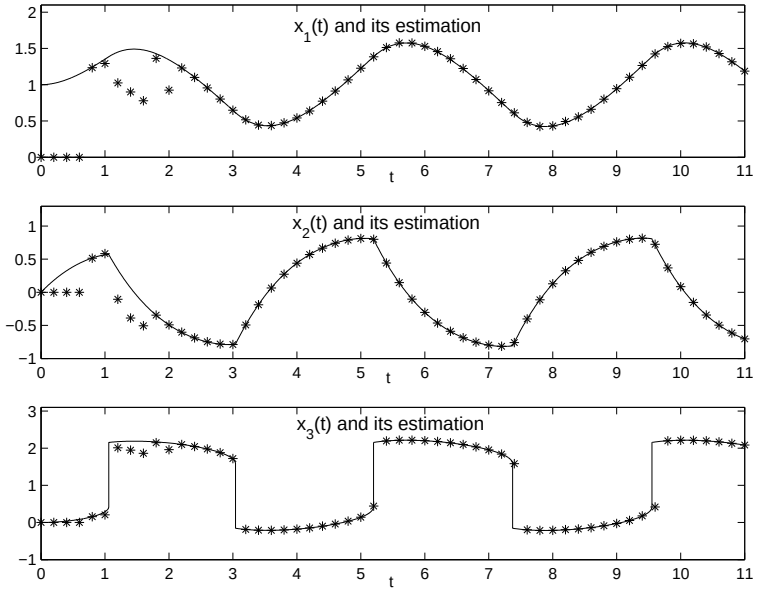

FIGURE 9. Performance of PS observer for system (41). The sampling period is 0.2 and the tuning parameters are $L = 5$ and $N = 15$. The solid lines are the real continuous states and '$*$' denotes the estimated states.

4. **Conclusion.** A pseudospectral observer is constructed in combination with a moving horizon strategy. The observer is proved to be convergent for a wide variety of nonlinear systems. A particularly important property of our proposed method is the fast convergent rate which makes the observer function as a numerical sensor. The observer algorithm is tested on a family of chaotic Duffing systems under uncertainty and measurement noise. The result presented in this paper also helps in the design of output feedback control for nonlinear control systems.

REFERENCES

[1] C. Canuto, M.Y. Hussaini, A. Quarteroni and T.A. Zang, "Spetral Method in Fluid Dynamics," Springer-Verlag, New York, 1988.

[2] G. Elnagar, M. A. Kazemi and M. Razzaghi, *The pseudospectral Legendre method for discretizing optimal control problems*, IEEE Trans. Automat. Contr., **40** (1995), 1793–1796.

[3] G. Freud, "Orthogonal Polynomials," Pergamon Press, 1971.

[4] J. P. Gauthier, H. Hammouri, and S. Othman, *A simple observer for nonlinear systems with applications to bioreactors*, IEEE Trans. Automat. Contr., **37** (1992), 875–880.

[5] Q. Gong, W. Kang and M. I. Ross, *A pseudospectral method for the optimal control of constrained feedback linearizable systems*, IEEE Trans. Automat. Contr., **51** (2006), 1115–1129.

[6] Q. Gong, I. M. Ross, W. Kang and F. Fahroo, *Connections between the covector mapping theorem and convergence of pseudospectral methods for optimal control*, to appear in Computational Optimization and Applications, 2007.

[7] Q. Gong, I. M. Ross, W. Kang and F. Fahroo, *On the pseudospectral covector mapping theorem for nonlinear optimal control*, 45th IEEE Conference on Decision and Control, San Diago, CA (2006), 2679–2686.

[8] Q. Gong, I. M. Ross and W. Kang, *A unified pseudospectral framework for nonlinear controller and observer design*, to appear in American Control Conference, New York, NY (2007).

[9] S. J. Julier and J. K. Uhlmann, *Unscented filtering and nonlinear estimation*, Proceedings of the IEEE, **92** (2004), 401–422.

[10] W. Kang, *Moving horizon numerical observers of nonlinear control systems*, IEEE Trans. Automat. Contr., **51** (2006), 344–350.

[11] W. Kang, Q. Gong and I. M. Ross, *Convergence of pseudospectral methods for a class of discontinuous optimal control*, 44th IEEE Conference on Decision and Control and European Control Conference (CDC-ECC'05), Seville, Spain (2005), 2799–2804.

[12] A. J. Krener and A. Isidori, *Linearization by output injection and nonlinear observers*, Systems and Control Letters, **27** (1983) 47–52.

[13] A. J. Krener and W. Kang, *Locally convergent nonlinear observers*, SIAM J. Control Optim., **42** (2003), 155–177.

[14] A. J. Krener and M. Xiao, *Observers for linearly unobservable nonlinear systems*, Systems and Control Letters, **46** (2002), 281–288.

[15] H. Michalska and D. Q. Mayne, *Moving horizon observers and observer-based control*, IEEE Trans. Automat. Contr., **40** (1995), 995–1006.

[16] P. E. Moraal and J. W. Grizzle, *Observer design for nonlinear systems with discrete-time measurements*, IEEE Trans. Automat. Contr., **40** (1995), 395–404.

[17] E. Polak, "Optimization: Algorithms and Consistent Approximations," Springer-Verlag, Heidelberg, 1997.

[18] C. V. Rao, J. B. Rawlings and D. Q. Mayne, *Constrainted state estimation for nonlinear discrete-time systems: stability and moving horizon approximations*, IEEE Trans. Automat. Contr., **48** (2003), 246–258.

[19] R. Riaza, *Double SIB points in differential-algebraic systems*, IEEE Trans. Automat. Contr., **48** (2003), 1625–1629.

[20] I. M. Ross and F. Fahroo, *Pseudospectral methods for optimal motion planning of differentially flat systems*, IEEE Transactions on Automatic Control, **49** (2004), 1410–1413.

[21] I. M. Ross and F. Fahroo, *Legendre pseudospectral approximations of optimal control problems*, Lecture Notes in Control and Information Sciences, **295** (2003), Springer-Verlag, 327–342.

[22] I. M. Ross and F. Fahroo, *A unified framework for real-time optimal control*, Proc. IEEE CDC, Maui, December (2003), 2210–2215.

Received August 2006; revised February 2007.

E-mail address: qi.gong@utsa.edu
E-mail address: imross@nps.edu
E-mail address: wkang@nps.edu